AD-A120 676

AD A-120676

TECHNICAL REPORT ARLCB-TR-82029

# FAILURE DESIGN OF THICK-WALLED CYLINDERS CONSIDERING THE OD AS A FAILURE INITIATION SITE


J. A. Kapp
S. L. Pu





September 1982

US ARMY ARMAMENT RESEARCH AND DEVELOPMENT COMMAND
LARGE CALIBER WEAPON SYSTEMS LABORATORY
BENÉT WEAPONS LABORATORY
WATERVLIET, N. Y. 12189

AMCMS No. 72801213000

PRON No. 1A1258731A1A


APPROVED FOR PUBLIC RELEASE; DISTRIBUTION UNLIMITED

## DISCLAIMER

The findings in this report are not to be construed as an official Department of the Army position unless so designated by other authorized documents.

The use of trade name(s) and/or manufacture(s) does not constitute an official indorsement or approval.

## DISPOSITION

Destroy this report when it is no longer needed. Do not return it to the originator.

SECURITY CLASSIFICATION OF THIS PAGE (*When Data Entered*)

# REPORT DOCUMENTATION PAGE

READ INSTRUCTIONS BEFORE COMPLETING FORM

| | |
|---|---|
| 1. REPORT NUMBER: ARLCB-TR-82029 | 2. GOVT ACCESSION NO. |
| 3. RECIPIENT'S CATALOG NUMBER | |
| 4. TITLE (*and Subtitle*): FAILURE DESIGN OF THICK-WALLED CYLINDERS CONSIDERING THE OD AS A FAILURE INITIATION SITE | 5. TYPE OF REPORT & PERIOD COVERED: Final |
| | 6. PERFORMING ORG. REPORT NUMBER |
| 7. AUTHOR(s): J. A. Kapp and S. L. Pu | 8. CONTRACT OR GRANT NUMBER(s) |
| 9. PERFORMING ORGANIZATION NAME AND ADDRESS: US Army Armament Research & Development Command, Benet Weapons Laboratory, DRDAR-LCB-TL, Watervliet, NY 12189 | 10. PROGRAM ELEMENT, PROJECT, TASK AREA & WORK UNIT NUMBERS: AMCMS No. 72801213000; PRON No. 1A1258731A1A |
| 11. CONTROLLING OFFICE NAME AND ADDRESS: US Army Armament Research & Development Command, Large Caliber Weapon Systems Laboratory, Dover, NJ 07801 | 12. REPORT DATE: September 1982 |
| | 13. NUMBER OF PAGES: 31 |
| 14. MONITORING AGENCY NAME & ADDRESS (*if different from Controlling Office*) | 15. SECURITY CLASS. (*of this report*): UNCLASSIFIED |
| | 15a. DECLASSIFICATION/DOWNGRADING SCHEDULE |

16. DISTRIBUTION STATEMENT (*of this Report*)

Approved for public release; distribution unlimited.

17. DISTRIBUTION STATEMENT (*of the abstract entered in Block 20, if different from Report*)

18. SUPPLEMENTARY NOTES

Presented at ASME Pressure Vessel Design Conference, Orlando, FL, June 1982. Published in proceedings of the conference.

19. KEY WORDS (*Continue on reverse side if necessary and identify by block number*)

Fatigue
Thick-Walled Cylinders
Fracture Mechanics
Crack Initiation
Crack Growth

20. ABSTRACT (*Continue on reverse side if necessary and identify by block number*)


The outside diameter (OD) of thick-walled pressure vessels is considered as the initiation site for fatigue failure of the cylinder. OD failures can occur in pressurized cylinders which have discontinuities machined on their outside surfaces, and have been strengthened by the autofrettage process. Both the crack initiation and crack propagation phases are discussed. To do this, finite element stress solutions for OD notched thick-walled cylinders and


(CONT'D ON REVERSE)

20. ABSTRACT (CONT'D)

specialized fracture mechanics solutions are presented. Life and crack growth predictions based on these analyses are compared to previously performed experiments.

TABLE OF CONTENTS



TABLES



LIST OF ILLUSTRATIONS

## INTRODUCTION

Thick-walled cylinders are often used to contain very high pressures.[1] The elastic stress solution for such cylinders was developed by Lamé and is well known (see for example, Reference 2). This solution shows that for a smooth cylinder the maximum stress occurs in the tangential direction at the inside diameter (ID). Such cylinders subjected to cyclic internal pressurization fail by crack initiation and growth from the ID.[3] To increase the fatigue life of cylinders, compressive residual stresses at the ID are often introduced by autofrettage.[4] As a result of the autofrettage, a tensile residual stress is induced at the OD. Sometimes after the autofrettage process, cylinders are machined on the OD producing stress concentrations, such as keyways, notches, holes, or threads. In these cylinders, the combination of tensile operating stress, tensile residual stress, and stress concentration often result in the OD, rather than the ID, being the fatigue failure initiation site.[5-7] OD initiated failures are less desirable since they occur often, but not exclusively accompanied by very little stable crack growth. Catastrophic failure occurs shortly after the initiation and coalescence of many short penny shaped cracks to form a shallow straight-fronted crack.[6]

OD discontinuities in thick cylinders have been the subject of several experimental[5-9] and theoretical[8,10-20] studies. The bulk of the experimental work[5-7,9] has dealt with the effects of stress concentrations of fatigue crack initiation, while one study has discussed crack growth from the OD. All of these studies were on cylinders which either had been autofrettaged[5-8] or were

References are listed at the end of this report.

loaded in such a way as to simulate the presence of autofrettage residual stresses. The theoretical work has included internally pressurized cylinders containing OD cracks,[8,10-12,14,15,20] autofrettaged cylinders with OD cracks,[16,19,20] and autofrettaged cylinders with stress concentrations at the OD.[13,17,18]

In the experimental studies, Brown[5] and Brown and McAlonie[6,7] have fatigue tested actual autofrettaged cannon barrels containing OD notches. Their results showed that these cylinders failed by crack initiation at the notches followed by very little crack growth before gross through thickness fracture. In an attempt to model this behavior experimentally, without the expense of testing large cannon barrels, Kapp and Underwood[9] have used a simulation specimen. This specimen was a modified C-shaped fracture toughness specimen,[21] with the same OD notch studied by Brown and McAlonie.[6] By loading this specimen properly, the same stresses were developed at the OD notch as occurred in the actual cylinder. The agreement with the fatigue data in Reference 6 was excellent. By using this specimen, design variables such as the degree of autofrettage or notch geometry could be tested very efficiently. These variables were tested and showed that fatigue life can be changed much more by modifying the stress concentration of the OD configuration, than by reducing the amount of autofrettage. In the other experimental study, Kapp and Eisenstadt[8] measured fatigue crack growth rates in autofrettaged rings with radial cracks emanating from the OD. The results showed that autofrettage could increase the fatigue crack growth rate by as much as an order of magnitude when compared to the results obtained in specimens which contained no autofrettage residual stresses.

The first theoretical study, by Emery and Segedin,[10] was a stress intensity factor, K, solution for thick- and thin-walled cylinders loaded by internal pressure using a finite difference method. When their solutions were compared to K solutions developed using finite elements[8,18,20] and mapping collocation solutions[14,16,19] the agreement was not good, although the finite element and collocation results normally agree within two percent. The initial collocation results[14] were for cylinders containing from one to four cracks loaded by internal pressure, with various diameter ratios, W, (W = OD/ID). The first finite element study[8] was for a single crack in a cylinder with W = 2.

Subsequent numerical K solutions[16,19,20] included autofrettage residual stresses and internal pressure for as many as 40 standard cracks in cylinders of various diameter ratios. Solutions for the autofrettage cases required the development of some specialized stress analysis techniques. Since autofrettage residual stresses exist in a cylinder under the action of no external active loads, the special stress analysis methods were needed. Two basic methods were developed, superposition and simulation. Using the superposition method,[16,19] a pressure was applied to the crack surfaces which was equivalent to the negative of the stress which would have acted at the same location in a cylinder with no crack present. In a modification of this, Pu[20] used a weight function approach which was somewhat different than the method used by Parker,[16,19] yielding the same results. Using the simulation technique[16,19,20] the autofrettage residual stresses were simulated through the use of an active thermal distribution. The method, developed independently by Parker and Farrow[22] and Hussain et al,[23] showed that a properly defined, loga-

rithmically varying temperature distribution produces exactly the same stress distribution as autofrettage in an uncracked cylinder. By applying this same temperature distribution to a cracked cylinder, the K solution developed agreed very well with the superposition solutions. Autofrettage resulted in very high K values, with the highest values resulting from the higher degrees of autofrettage. Also, the most severe case occurred when there were two diametrically opposed cracks.

The theoretical studies on notched cylinders[13,17,18] are much less extensive than on cracked cylinders. In the first paper,[13] stresses in OD notches were estimated, while in the more involved studies,[17,18] the stresses were calculated using the finite element method and the thermal loading simulation method.[22,23] The solutions showed that the OD notches studied concentrated the stress to the extent that the notches became the highest stressed point in the cylinder, even if the cylinder was not autofrettaged. The autofrettage results indicated that stresses exceeding the yield strength of the cylinder material acted at the OD notches. Furthermore, the presence of the notches relieved the autofrettage residual stresses throughout the cylinder by as much as 30 percent.

In this report we will attempt to relate the theoretical and experimental work that has been performed to develop a guideline that may be used in the design of thick-walled cylinders containing OD discontinuities. The discussion will involve three main areas: special stress analysis methods, failure by fatigue crack initiation, and failure by fatigue crack growth.

## STRESS ANALYSIS

A thick-walled cylinder of radius ratio (b/a) of two is shown in Figure 1, which also defines the geometric parameters used in the equations below. Three loading conditions will be discussed: internal pressure, autofrettage, and diametrical line loading used in the fatigue crack growth measurements of Reference 8. The three loading conditions are shown schematically in Figure 2.

For a thick-walled cylinder subjected to internal pressure, the stresses follow the well known Lamé distributions[2]

$$\sigma_\theta = \frac{pa^2}{b^2-a^2}\left(1 + \frac{b^2}{r^2}\right) \tag{1}$$

$$\sigma_r = \frac{pa^2}{b^2-a^2}\left(1 - \frac{b^2}{r^2}\right) \tag{2}$$

where p is the internal pressure and the subscripts $\theta$ and r signify the tangential and radial directions respectively.

For the case of autofrettage, the stress distributions in a smooth cylinder are somewhat more complex than equations (1) and (2). These autofrettage stresses result from loading the cylinder with sufficient pressure to cause plastic deformation to some extent through the thickness of the cylinder. The degree of autofrettage is measured by the elastic-plastic radius, $\rho$. This is the radius at which, under the loading of the autofrettage pressure, yielding of the material is just occurring. The value of $\rho$ gives a measure of the amount of autofrettage defined as percent overstrain (% overstrain = 100 x$(\rho-a)/t$). The general solutions for the autofrettage residual stresses calculated assuming elastic, perfectly plastic material behavior and

the Tresca yield criteria are:[1]

$$\sigma_\theta = \begin{cases} \sigma_o\{\dfrac{a^2}{b^2-a^2}[1+\dfrac{b^2}{r^2}][\dfrac{\rho^2-b^2}{2b^2} - \ln\dfrac{\rho}{a}] + [\dfrac{\rho^2+b^2}{2b^2} - \ln\dfrac{\rho}{r}]\} & a < r < \rho \\ \\ \sigma_o[1+\dfrac{b^2}{r^2}]\{\dfrac{\rho^2}{2b^2} + \dfrac{a^2}{b^2-a^2}[\dfrac{\rho^2-b^2}{2b^2} - \ln\dfrac{\rho}{a}]\} & \rho < r < b \end{cases} \tag{3}$$

$$\sigma_r = \begin{cases} \sigma_o\{\dfrac{a^2}{b^2-a^2}[1-\dfrac{b^2}{r^2}][\dfrac{\rho^2-b^2}{2b^2} - \ln\dfrac{\rho}{a}] + [\dfrac{\rho^2+b^2}{2b^2} - \ln\dfrac{\rho}{r}]\} & a < r < \rho \\ \\ \sigma_o[1+\dfrac{b^2}{r^2}]\{\dfrac{\rho^2}{2b^2} + \dfrac{a^2}{b^2-a^2}[\dfrac{\rho^2-b^2}{2b^2} - \ln\dfrac{\rho}{a}]\} & \rho < r < b \end{cases} \tag{4}$$

where $\sigma_o$ is the tensile yield strength. It is important to note that the autofrettage residual stresses act in the cylinder under no active external loads. This causes some problems when attempting to determine the effects of structure discontinuities on autofrettaged cylinders.

Under the diametrical line loading, the stresses can be calculated exactly only in the form of an infinite series.[24] The solutions for thick cylinders of radius ratio, W, (W = b/a) ranging from 2 to 10 have been developed by Rigsperger and Davis.[25] For the purpose of this report, the stress which acts at the OD for a cylinder with W = 2 is given. This stress acting 90° removed from the load is:

$$\sigma_\theta = \frac{5.88F}{\pi b} \tag{5}$$

where F is the total force which acts at the OD as shown in Figure 2.

To determine the effects of OD discontinuities on the stresses given above, accurate numerical techniques must be used which incorporate such

discontinuities. Three such methods have been used to do this, a finite difference method, the finite element method, and the boundary collocation mapping technique. The finite difference approach[10] was used to determine stress intensity factor, K, solutions for thick-walled cylinders of various W with a single OD crack. The solutions, when compared with K solutions developed using finite elements[8,20] and the collocation method[14,16,19] were inferior. More accurate K solutions were developed using the latter two methods. Accurate K solutions are necessary when predicting the rate of growth of stable fatigue cracks and unstable fracture.

To develop K solutions using the finite element method, it is the stress singularity at the crack tip which causes difficulties. A very large number of elements is usually required near the crack tip to represent the steep strain gradient. The recent trend in finite element method is to use high order isoparametric elements[26] so that a high degree of accuracy may be achieved with a small number of elements. This trend calls for special elements[27,28] which can produce the proper order of singular stresses and strains at a crack tip. The enriched elements[27] that contain $K_I$ and $K_{II}$ as additional unknowns are used to model the crack tip region. The approximate values of $K_I$ and $K_{II}$ are directly obtained together with nodal displacements. The collapsed elements,[28,29] on the other hand, compute the nodal displacements first. Since a correct order of strain singularity is built in the special crack tip elements, the displacements obtained are quite accurate. The stress intensity factors are indirectly calculated from the near field elasticity solution of displacements in terms of stress intensity factors. Both enriched elements and collapsed elements yield comparably accurate K

values.

In the modified boundary collocation[14] method, the geometry of the physical structure is mapped through the use of a complex mapping function to a simpler geometry in a complex plane. The stress analysis is then performed in the complex plane and the solution to the physical problem is obtained by using the same complex mapping function to return to physical space. To use this method on cylinder problems, the cracked cylinder is first mapped to a square or rectangular cracked plate. The plate in turn is mapped to a geometry where the crack is represented by a semicircle. Therefore, two mappings must be used to obtain the solution. This method was used to determine K for one to four OD cracks in cylinders which had two W values loaded with internal pressure.[14] The K solutions for one external crack with internal pressure loading are shown in Table I.

To use the stress analysis techniques described above, the finite element model or the mapped geometry must be loaded by active loads. Since the autofrettage stresses act in the absence of such active external loads, K solutions were developed using the superposition or the thermal loading simulation techniques described above. Superposition is more often used with the mapping collocation method, while the simulation method is more often used with the finite element methods. The agreement between the collocation[19] and finite element[20] solutions was not as good as would have been expected (about five percent difference). This was attributed to relatively coarse finite element grid used in Reference 20. The results for a radius ratio of two and a single external crack for autofrettage loading are shown in Table I.

TABLE I. K SOLUTIONS FOR EXTERNALLY CRACKED THICK-WALLED CYLINDERS

(See Table II for the definition of $\sigma_{OD}$)

Internal Pressure, 1 Crack

$$\frac{K}{\sigma_{OD}\sqrt{\pi c}}$$

| c/t | W=2, FE[8] | c/t | W=2, COL[14] | W=3, COL[14] |
|---|---|---|---|---|
| 0.167 | 1.341 | 0.1 | 1.20 | 1.23 |
| 0.250 | 1.465 | 0.2 | 1.37 | 1.37 |
| 0.333 | 1.635 | 0.3 | 1.56 | 1.54 |
| 0.417 | 1.883 | 0.4 | 1.80 | 1.82 |
| 0.500 | 2.102 | 0.5 | 2.10 | 2.12 |
| 0.583 | 2.404 | 0.6 | 2.49 | 2.43 |
| 0.667 | 2.753 | 0.7 | - | 3.11 |
| 0.750 | 3.247 | | | |
| 0.833 | 3.458 | | | |

Autofrettage, 1 Crack

$$\frac{K}{\sigma_{OD}\sqrt{\pi c}}, \quad W = 2$$

| c/t | 50% Overstrain | 100% Overstrain |
|---|---|---|
| 0.1 | 1.129 | 1.013 |
| 0.2 | 1.235 | 0.977 |
| 0.3 | 1.424 | 0.969 |
| 0.4 | 1.647 | |
| 0.5 | 1.924 | |
| 0.6 | 2.041 | 0.923 |

To use the numerical solutions given in Table I to predict the rate of growth of fatigue cracks or fracture, K should be known as a continuous function of crack length. This can be accomplished by fitting a polynomial to the numerical K solutions along with limiting solutions.[30] The expressions that were developed for some of the numerical results in Table I have the form

$$K = \sigma_{OD} \sqrt{\pi c}(1.12 + A_1(c/t) + A_2(c/t)^2 + A_3(c/t)^3 + A_4(c/t)^4)$$

where $\sigma_{OD}$ is the stress which acts at the OD of an uncracked cylinder due to the applied loading; $A_1$, $A_2$, $A_3$ and $A_4$ are constants; c is crack length; and t is wall thickness (b-a). The factor 1.12 arises from the fact that as c approaches zero, K approaches the following:[31]

$$K = 1.12\ \sigma_{OD} \sqrt{\pi c} \qquad (6)$$

The values of the constants for various loadings are given in Table II for the cases of internal pressure, diametrical line loading, 50 percent overstrain and 100 percent overstrain, for a cylinder with W = 2 and a single external crack. These expressions represent the numerical results within three percent for any of the loadings considered.

As stated previously, there have been fewer theoretical studies on thick cylinders which contain OD discontinuities, such as notches, rather than cracks on the OD. In these studies, the stresses have been calculated by either estimation[13] or with finite elements.[17,18] The most extensive work[17] studied the case of a thick cylinder with W = 1.74, subjected to either internal pressure, 100 percent overstrain or 60 percent overstrain. The cylinder contained a single OD notch which had a root radius to thickness ratio (R/t) of 0.013, and a depth to thickness ratio (d/t) of either 0.088 or

TABLE II. COEFFICIENTS FOR THE EXPRESSIONS FOR THE STRESS INTENSITY FACTORS

$$K = \sigma_{OD}(\sqrt{\pi c}(1.12 + A_1(c/t) + A_2(c/t)^2 + A_3(c/t)^3 + A_4(c/t)^4)$$

| Loading Condition | $A_1$ | $A_2$ | $A_3$ | $A_4$ |
|---|---|---|---|---|
| Internal Pressure[8] | 0.31 | 6.85 | -12.12 | +10.02 |
| Diametrical Lineload[8] | -1.14 | 1.23 | - 2.20 | 0.0 |
| 50% Overstrain | 0.0 | 0.0 | 16.9 | -21.0 |
| 100% Overstrain | -1.44 | +4.444 | - 4.31 | 0.0 |

| Loading Condition | $\sigma_{OD}$ |
|---|---|
| Internal Pressure | $\dfrac{2pa^2}{b^2-a^2}$ |
| Diametrical Load | $\dfrac{5.88F}{\pi b}$ |
| 50% | $\dfrac{2\sigma_o}{\sqrt{3}}\left(\dfrac{x}{4} + \dfrac{1}{w^2-1}\left(\dfrac{x}{4} - 1 - 2\ell n\left(\dfrac{w+1}{2}\right)\right)\right), \; x = \left(1 + \dfrac{1}{w}\right)^2$ |
| 100% | $\dfrac{2\sigma_o}{\sqrt{3}}\left(1 + \dfrac{2\ell n\, w}{w^2-1}\right)$ |

0.177. The results of the finite element calculations are given in Table III. These show that the notches constitute a significant stress concentration which produced a stress concentration factor $k_t$ as high as 6.6 in the case of the deep notch, 100 percent overstrain condition. Another interesting finding of the study was that the presence of the notch caused a reduction or a redistribution of the autofrettaged residual stresses throughout the cylinder. Therefore, also included in Table III are the relief factors $R_s$, which are the ratios of the remaining residual stress to the residual stresses which acted in the cylinder prior to the introduction of the notch. To use the factors in Table III to calculate the stresses which act at the OD notch the following expression is used:

$$\sigma_{notch} = R_s \; k_t \; \sigma_\theta(r = b-d) \qquad (7)$$

where $\sigma_\theta(r)$ is given by equation (3).

TABLE III. STRESS CONCENTRATION FACTORS $k_t$ AND STRESS RELIEF FACTORS $R_s$ FOR AN OD NOTCHED CYLINDER, W = 1.74, ROOT RADIUS OF THE NOTCH = 0.013 t

| Loading Condition | Deep Notch (Depth=0.178 t) | | Shallow Notch (Depth=0.088 t) | |
|---|---|---|---|---|
| | $k_t$ | $R_s$ | $k_t$ | $R_s$ |
| Internal Pressure | 5.4 | - | 3.5 | - |
| 60% Overstrain | 5.8 | 0.71 | 3.5 | 0.72 |
| 100% Overstrain | 6.6 | 0.70 | 3.7 | 0.70 |

PREDICTING THE FAILURE OF CYLINDERS WITH OD DISCONTINUITIES

Using the results from the various stress analyses described above, we will attempt to predict failure under fatigue conditions. These failures can occur by either of two mechanisms, fatigue crack initiation, or fatigue crack growth. In the case of crack initiation, three factors contribute to failure, the alternating stress from external loading, tensile mean stress from the autofrettage stresses, and the stress concentration from the OD discontinuity. For failure by fatigue crack growth, two factors must be considered, the alternating K from the applied loading and the ratio of minimum K ($K_{min}$) to maximum K ($K_{max}$), during fatigue due to changes in autofrettage conditions. Crack initiation is considered first.

To predict fatigue crack initiation a parameter must be developed which includes all three of the contributing factors described above. Fuchs[32] has proposed such a parameter for predicting crack initiation at long life ($>10^6$ cycles). He states that if the following equation is valid crack initiation occurs:

$$\sigma_e \leq \frac{k_f}{\sqrt{2}} \left(\frac{\Delta\sigma}{2} + C\sigma_m\right) \qquad (8)$$

where $\sigma_e$ is the endurance limit of the material, $k_f$ is the fatigue stress concentration factor, $\Delta\sigma$ is the range of stress applied ($\Delta\sigma = \sigma_{max} - \sigma_{min}$), C is constant with a value of about 0.5, and $\sigma_m$ is the mean stress ($\sigma_m = (\sigma_{max} + \sigma_{min})/2$).

Extending Fuch's[32] work to short life situations (< $10^6$ cycles), it is assumed that the value of stress predicted by the right-hand side of equation (8) is equivalent to the uniaxial alternating stress which results in less than $10^6$ cycles. The relationship between the stress and life is determined by the S-N property of the material studied. The S-N behavior of a steel can be estimated to a first order approximation using the following assumptions.[33] At a life of $10^3$ cycles, a specimen in a compression-tension fatigue test will fail with an alternating stress of

$$\sigma_a = \frac{\Delta\sigma}{2} = 0.9\ \sigma_{uts}\ (@\ N = 10^3\ \text{cycles}) \qquad (9)$$

where $\sigma_{uts}$ is the ultimate tensile strength of the material. At a life of $10^6$ cycles, the allowable alternating stress is approximated as

$$\sigma_a = \frac{\Delta\sigma}{2} = 0.5\ k_a k_b k_c\ \sigma_{uts} \qquad (10)$$

where $k_a$ is a factor related to surface finish, $k_b$ is a factor related to the size of the component considered, and $k_c$ is a reliability factor dealing with statistical considerations. Assuming the steels considered have an ultimate tensile strength of about 1250 MPa, the cylinders have a machined finish and are larger than 2 cm, and we desire 99 percent reliability, the respective values of $k_a$, $k_b$, and $k_c$ are 0.65, 0.85, and 0.868. Equation (10) then becomes

$$\sigma_a = \frac{\Delta\sigma}{2} = 0.24\ \sigma_{uts}\ (@\ N = 10^6\ \text{cycles}) \qquad (11)$$

It is also assumed that the S-N property of the material falls on the straight line in log S-log N space which connects the two points defined by

equations (9) and (11). The solid line in Figure 3 is the estimated S-N property of the material. The data points in the same figure are actual measurements of fatigue life from References 8 and 9 using Fuch's criterion (Equation (8)). The stress concentration factors for the data from Reference 9 are from Reference 17 and are considered to be quite accurate. For the data from Reference 8, the stress concentration factors were estimated using a Nuber diagram,[34] and are considered less accurate than those calculated in Reference 17.

The comparison of the available data with the estimated fatigue life to crack initiation suggests that the procedure outlined above is conservative if the stress concentration factors are known accurately. If the stress concentration factors must be estimated, the failure prediction gives an approximate average of failure. In some cases life is underestimated, in others it is overestimated. To use this method in design warrants the use of safety factors if $k_t$ is not accurately known. The dotted line in Figure 4 shows the failure prediction using a safety factor of two on stress. In this instance, all of the data fall well beyond the predicted failure curve when $k_t$ is estimated. Using safety factors should only be applied when $k_t$ is estimated, since they may be overly restrictive when $k_t$ is accurately known.

To predict failure by fatigue crack growth, a crack growth law which is a property of the material is needed. The first law developed was the well known Paris power law[35]

$$\frac{dc}{dN} = C_1 \cdot \Delta K^m \tag{12}$$

where $C_1$ and m are constants, dc/dN is the measured fatigue crack growth rate, and $\Delta K$ is the range of stress intensity factor applied during loading. This law is useful in predicting crack growth if K ranges from zero to a positive value. If K varies from a positive value, $K_{min}$, to a maximum value, $K_{max}$, the crack growth rate may be different from that predicted using equation (12). This is the case when considering the effect of autofrettage on crack growth.[8]

To model the effects of cycling between two positive K values, several laws have been suggested. These laws have also incorporated static properties of the material in their formulation. Either of two static properties, fracture toughness, $K_{Ic}$, or yield strength, $\sigma_o$ are used. A crack growth law using $K_{Ic}$ is of the form[36]

$$\frac{dc}{dN} = \frac{C_2 \Delta K^m}{\{(1-R_f)K_{Ic} - \Delta K\}} \tag{13}$$

where $C_2$ and m are constants and $R_f$ is the ratio of minimum K to maximum K ($R_f = K_{min}/K_{max}$).

An example of a crack growth law incorporating the yield strength of the material is due to Tabeshfar and Williams:[37]

$$\frac{dc}{dN} = C_3\left(\frac{K_{max}}{\sigma_o}\right)^m \tag{14}$$

where $C_3$ and m are constants.

We used these laws to predict crack growth through the autofrettaged cylinders reported in Reference 8. The material used in that study was an AISI 4340 steel with yield strength of about 1140 MPA, and $K_{Ic}$ of about 150 $MPa\sqrt{m}$. The fatigue crack growth property (Equation (12)) has been measured for this material.[38] Using these data the constants in all the crack growth

laws can be determined. For the Paris,[35] Forman et al,[36] and the Tabeshfar and Williams[37] models respectively, the crack growth laws are:

$$\frac{dc}{dN} = 2.46 \times 10^{-6}\ \Delta K^{2.1} \tag{15}$$

$$\frac{dc}{dN} = \frac{4.80 \times 10^{-8}\ \Delta K^{2}}{\{150(1-R_f) - \Delta K\}} \tag{16}$$

$$\frac{dc}{dN} = 2.71 \times 10^{-10}\ K_{max}{}^{2.1} \tag{17}$$

All of these growth laws are variable separable differential equations of the form

$$\frac{dc}{dN} = F(K,R_f,\ldots) \tag{18}$$

To make crack growth predictions the crack growth laws must be integrated to give a function which relates crack length to number of cycles, N. This is accomplished by rearranging equation (18) to

$$dN = \frac{dc}{F(K,R_f,\ldots)} \tag{19}$$

Equation (19) is now in a form which can be easily integrated using numerical techniques, the simplest being the trapezoidal rule.[39]

In Reference 8 crack growth measurements were obtained in cylinders which were not autofrettaged or autofrettaged to either 50 percent or 100 percent overstrain. All three crack growth laws were used to predict crack growth under all three of the imposed testing conditions, using the stress intensity factor expressions from Table II to calculate the required K relationships for the predictions. The results are shown in Figures 4, 5, and

6 for the non-autofrettaged, 50 percent overstrain and 100 percent overstrain conditions respectively.

For the case of no autofrettage, Figure 4, it is clear that all three crack growth models adequately model the reported crack growth from Reference 8. There is an ordering of the crack growth predictions which shows that the Paris model predicts the slowest crack growth, the Tabeshfar and Williams the fastest and the Forman et al falling in between giving the best approximation to the actual behavior. This suggests that there is an effect of $R_f$ ratio even in the case of no autofrettage when one would consider the Paris law to provide the best prediction. In the experiments reported in Reference 8, $R_f$ was 0.1, while the crack growth data from Reference 7 was developed with $R_f = 0$.

In examining the results in autofrettage cylinders, Figures 5 and 6, we find that no model gives an accurate estimate of fatigue crack growth. The poorest correlation occurs in the case of 100 percent overstrain, where the Tabeshfar and Williams model predicts the crack should grow to a length of about 9.5 mm in less than 2,500 cycles when it actually required about 50,000 cycles to obtain that depth. To explain this difference it should be noted that in the initial crack growth regions, the Paris model gives a relatively good approximation for the crack growth behavior. At greater crack depths, the Paris prediction substantially overestimates the cycles required to grow the crack further. Although the Forman et al, and Tabeshfar and Williams models underestimate the crack growth behavior initially, the cycles required to cause additional crack growth are reasonably approximated. For example consider the 50 percent overstrain case, Figure 5. To grow a crack from 4 mm

to about 7.5 mm requires about 15,000 cycles according to Forman et al. In the data from Reference 8 for the same range of crack growth, 25,000 to 30,000 cycles were actually needed. These observations suggest that near the starter notch used to initiate the fatigue cracks, a model assuming no autofrettage applies, while removed from the starter notch, a model which incorporates a significant contribution from autofrettage seems to give a reasonable estimate of life. This indicates that the presence of the notch may significantly change the residual stresses near the notch. Removed from the notch, there seems to be little effect on the residual stress due to the notch; the crack growth model of Forman et al gives a reasonable estimate of crack growth.

## CONCLUSIONS

Much work, mostly theoretical stress analyses, has been performed to study the effects of OD initiated failures in thick-walled cylinders. The stress analyses were developed using very accurate numerical techniques which have the potential for being very useful in the design of thick-walled pressure vessels. At this time there seems to be insufficient experimental results to use the theoretical studies to predict the OD initiated failure of these vessels with any great accuracy. Using the analytical results and estimated fatigue crack initiation properties, conservative estimates of fatigue life can be made which may be useful to prepare cylinder designs which should not fail by fatigue crack initiation. Also, if failure occurs by fatigue crack growth, conservative estimates of fatigue life may be obtained using available crack growth models. Neither of the two models which account for the mean stress affect on fatigue crack growth agreed very well with the

observed data. The use of the model by Forman et al[36] did give the best estimate of the maximum fatigue crack growth rates and should give a conservative estimate of fatigue life. More work is needed to develop the technology necessary to estimate fatigue failure with greater accuracy.

## REFERENCES


1. Davidson, T. E. and Kendall, D. P., The Mechanical Behavior of Materials Under Pressure, H.L.I.D. Pugh, Ed., Elsevier Publishing, Amsterdam, 1970.
2. Harvey, John F., Theory and Design of Modern Pressure Vessels, 2nd Ed., Van Nostrand Reinhold Co., New York, 1974, p. 59.
3. Davidson, T. E., Eisenstadt, R., and Reiner, A. N., ASME Journal of Basic Engineering, December 1963, p. 555.
4. Davidson, T. E., Barton, C. S., Reiner, A. N. and Kendall, D. P., in Proceedings of the First International Congress on Experimental Mechanics, Pergamon Press, Oxford, 1963.
5. Brown, Bruce B., "Fatigue Test, 155 MM M199 Barrel," ARRADCOM Technical Report ARLCB-TR-80034, Benet Weapons Laboratory, Watervliet, NY, December 1980.
6. Brown, Bruce B. and McAlonie, Howard D., "Safe Service Life Testing of the 155 MM M185 Howitzer Barrel With M203 Propelling Charge," ARRADCOM Technical Report ARLCB-TR-81032, Benet Weapons Laboratory, Watervliet, NY, August 1981.
7. Brown, Bruce B. and McAlonie, Howard D., "Fatigue Performance Comparison of Rotary Forged and Conventionally Forged Cannon Barrels (105 MM M68)," ARRADCOM Technical Report ARLCB-TR-81037, Benet Weapons Laboratory, Watervliet, NY September 1981.
8. Kapp, J. A. and Eisenstadt, R., in Fracture Mechanics, Smith, C. W., Ed., ASTM STP 677, American Society of Testing and Materials, Philadelphia, PA, 1979, p. 746.

9. Kapp, J. A. and Underwood, J. H., Proceedings of the Third International Congress on Experimental Mechanics, Society for Experimental Stress Analysis, Brookfield Center, CT, 1981.

10. Emery, A. F. and Segedin, C. M., Journal of Basic Engineering, June 1972, p. 387.

11. Chapra, P. S., Nuclear Engineering Design, Vol. 29, 1974, p. 7.

12. Kobayashi, A. S., Polvanich, N., Emery, A. F., and Love, W. J., Journal of Pressure Vessel Technology, February 1977, p. 83.

13. Hussain, M. A. and Pu, S. L., "Preliminary Study of the Effect of a Recoil Keyway on the Fatigue Life of the M185 Cannon Tube," ARRADCOM Technical Report ARLCB-TR-78017, Benet Weapons Laboratory, Watervliet, NY, 1978.

14. Tracy, P. G., Engineering Fracture Mechanics, Vol. 11, 1979, p. 291.

15. Cesari, Francesco, and Hellen, T. K., International Journal of Pressure Vessels and Piping, Vol. 7, 1979, p. 199.

16. Parker, A. P. and Andrasic, C. P., "Stress Intensity Prediction for a Multiply-Cracked, Pressurized Gun Tube With Residual and Thermal Stresses," presented at the Army Symposium on Solid Mechanics, 1980.

17. Kapp, J. A. and Pflegl, G. A., Journal of Pressure Vessel Technology, Vol. 103, February 1981, p. 78.

18. Pu, S. L. and Hussain, M. A., Journal of Pressure Vessel Technology, Vol. 103, May 1981, p. 301.

19. Parker, A. P., "Stress Intensity and Fatigue Crack Growth in Multiply-Cracked, Pressurized Partially Autofrettaged Thick Cylinders," AMMRC Technical Report TR81-37, 1981.

20. Pu, S. L., "Stress Intensity Factors for Radial Cracks at Outer Surface of a Partially Autofrettaged Cylinder Subjected to Internal Pressure," ARRADCOM Technical Report ARLCB-TR-82002, Benet Weapons Laboratory, Watervliet, NY, 1982.

21. Underwood, J. H. and Kendall, D. P., Developments in Fracture Mechanics Test Methods, ASTM STP 632, 1977, p. 25.

22. Parker, A. P. and Farrow, J. R., Journal of Strain Analysis, Vol. 15, No. 1, 1980, p. 51.

23. Hussain, M. A., Pu, S. L., Vasilakis, J. D., and O'Hara, G. P., Journal of Pressure Vessel Technology, Vol. 102, No. 3, 1980, p. 314.

24. Timoshenko, S. P. and Goodier, J. N., Theory of Elasticity, 3rd Ed., McGraw-Hill, NY, 1970, p. 136.

25. Rigsperger, E. A. and Davis, N., Trans. ASCE, Vol. 112, 1947, p. 619.

26. Gifford, I. N., Jr., "APES-Second Generation Two-Dimensional Fracture Mechanics and Stress Analysis by Finite Elements," Report 4799, Naval Ship Research and Development Center, 1975.

27. Gifford, I. N., Jr. and Hilton, P. D., "Stress Intensity Factors by Enriched Finite Elements," Engineering Fracture Mechanics, Vol. 10, No. 3, 1978, pp. 485-496.

28. Barsoum, R. S., International J. for Numerical Methods in Engineering, Vol. 10, 1976, p. 25.

29. Pu, S. L., Hussain, M. A., and Lorensen, W. E., "The Collapsed Cubic Isoparametric Element as a Singular Element for Crack Problems," Int. J. for Numerical Methods in Engineering, Vol. 12, 1978, pp. 1727-1742.

30. Kapp, J. A., Newman, J. C., Jr., and Underwood, J. H., Journal of Testing and Evaluation, Vol. 8, No. 6, November 1980, p. 314.

31. Tada, H., Paris, P. C., and Irwin, G. R., The Stress Analysis of Cracks Handbook, Del Research Corp., Hellertown, PA, 1973.

32. Fuchs, H. D., J. of Basic Engineering, Series D, Vol. 87, 1965, p. 333.

33. Shigley, Joseph Edward, Mechanical Engineering Design, McGraw-Hill, NY, 1972, p. 245.

34. Ugural, A. C. and Feuster, S. K., Advanced Strength and Applied Elasticity, American Elsevier Publishing Co., NY, 1975, p. 83.

35. Paris, P. and Erdogan, F. J., J. of Basic Engineering, Vol. 85, Series D, 1963, p. 5280.

36. Forman, R. G., Kearney, V. E. and Engle, R. M., J. of Basic Engineering, Vol. 89, Series D, 1967, p. 459.

37. Tabeshfar, K. and Williams, T. R. G., J. of Sound and Vibration, Vol. 68, No. 2, 1980, p. 295.

38. Damage Tolerant Design Handbook, Part 2, Metals and Ceramics Information Center, Battelle, Columbus, OH, January 1975.

39. Carnahaw, Bruce, Luther, H. A., and Wilkes, James O., Applied Numerical Methods, John Wiley & Sons, Inc., New York, 1969, p. 73.

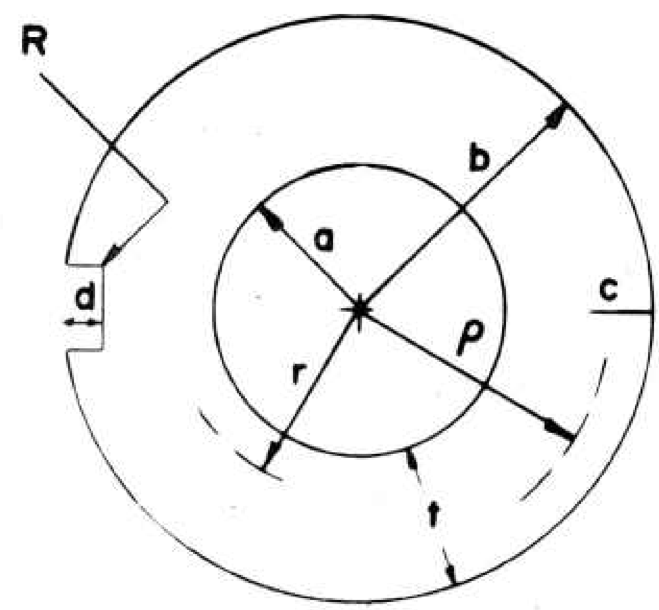


Figure 1. A Thick-Walled Cylinder Containing Various OD Discontinuities.

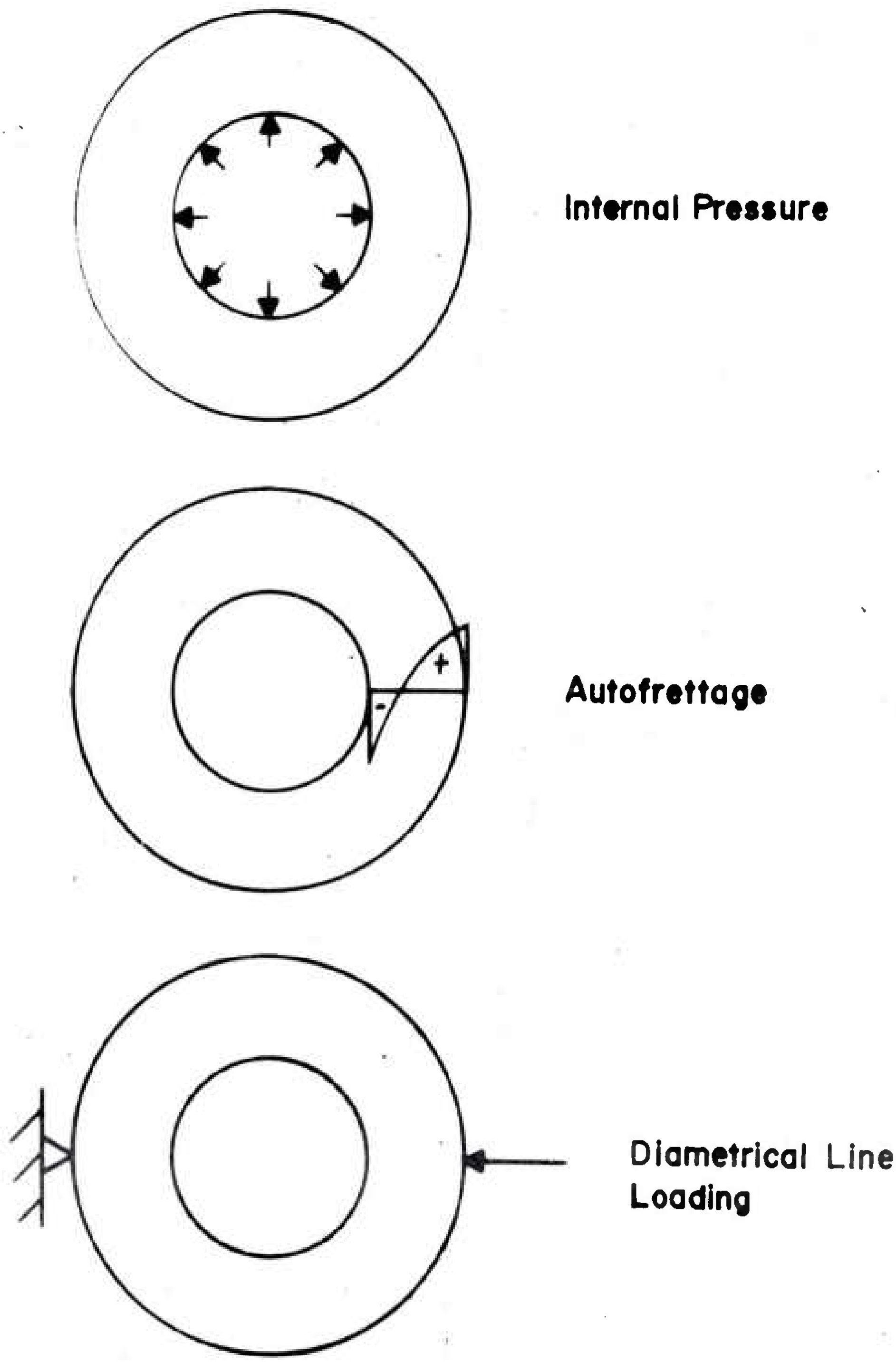


Figure 2. The Three Loading Conditions Considered.

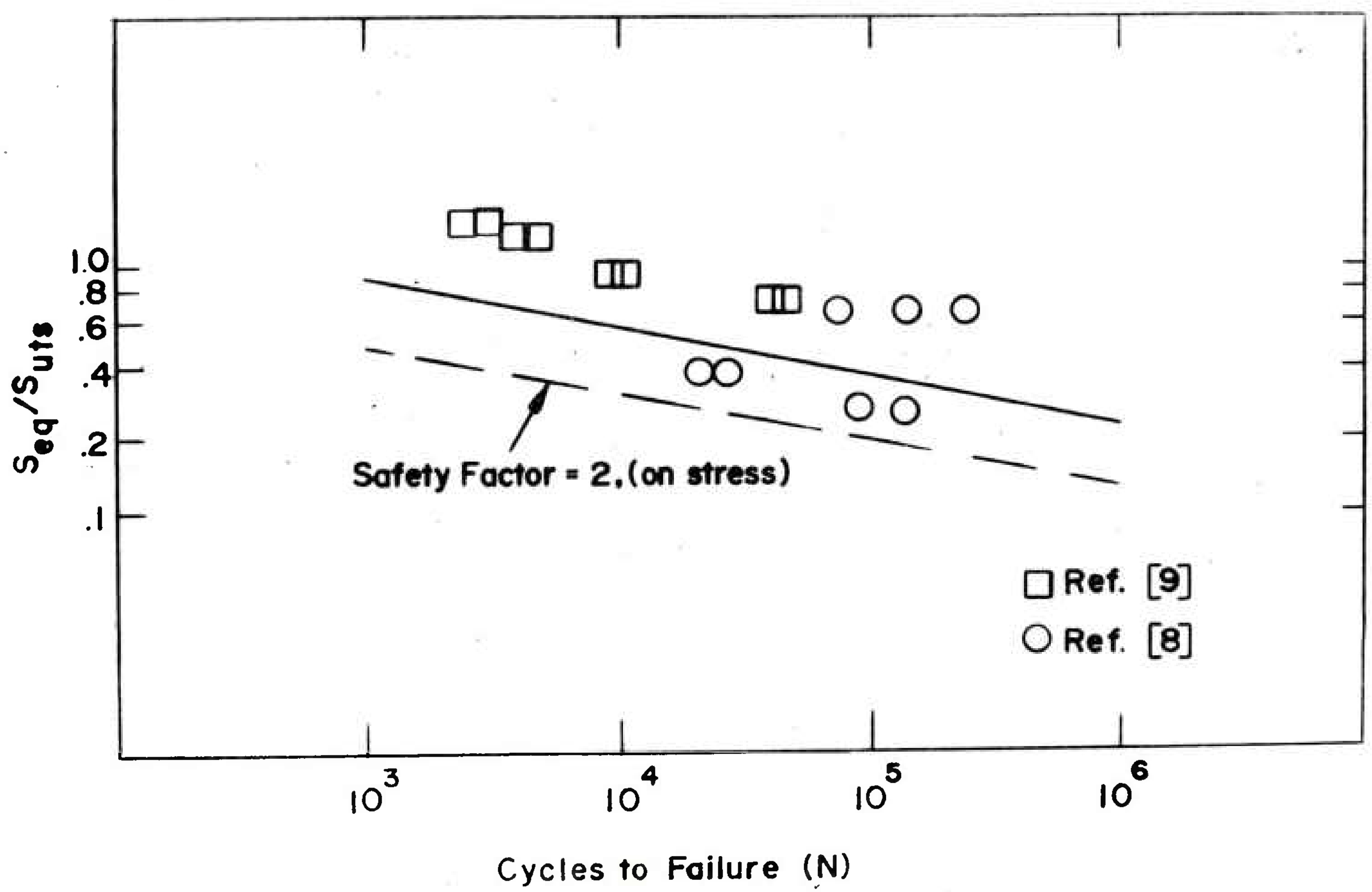


Figure 3. Comparison of Measured Fatigue Life and the Estimated Fatigue Life Expanding on Fuch's Crack Initiation Criteria.[32]

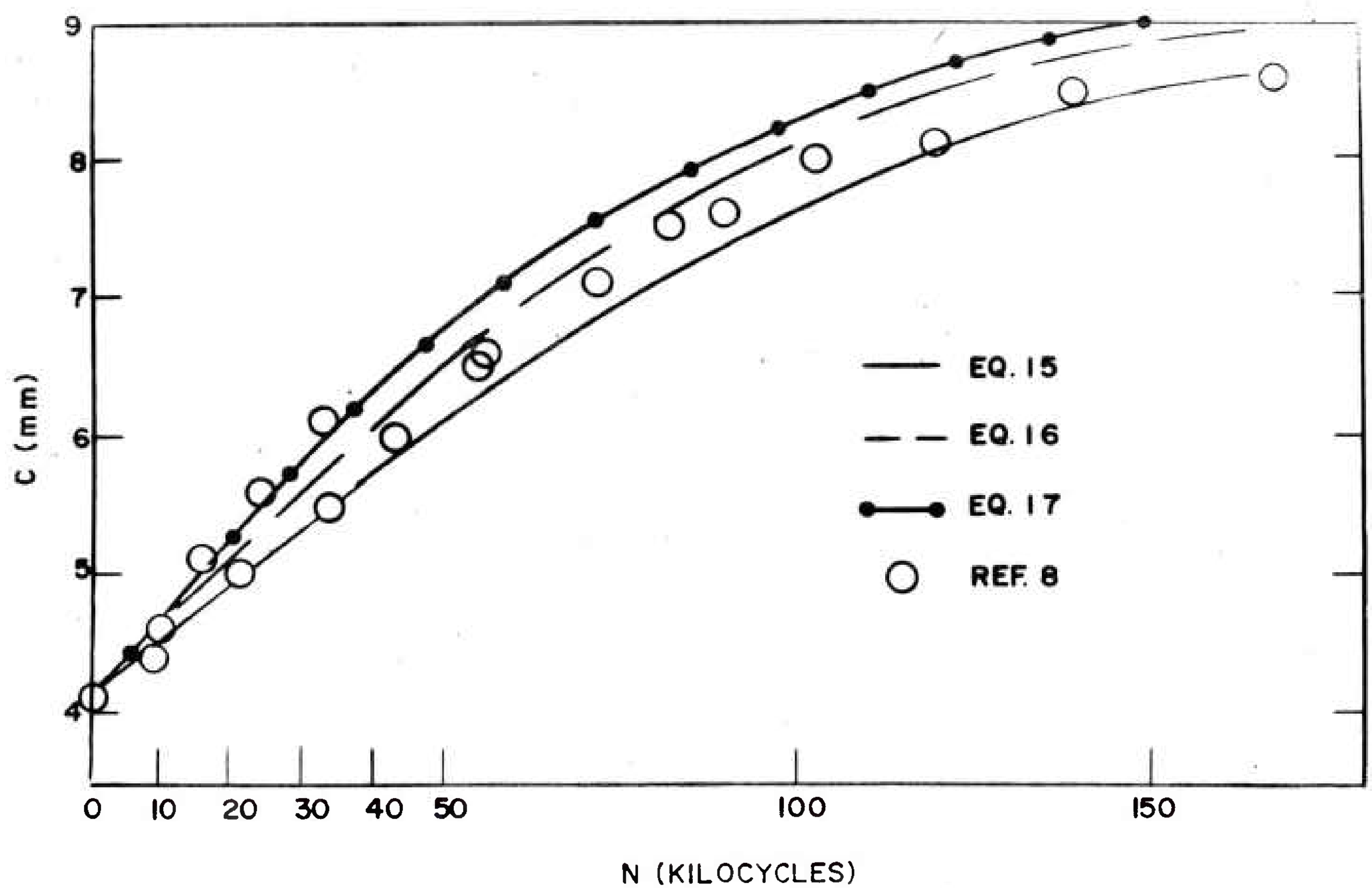


Figure 4. Comparison of Measured Fatigue Crack Growth and Predicted Fatigue Crack Growth Using Various Models for a Cylinder Containing No Residual Stress.

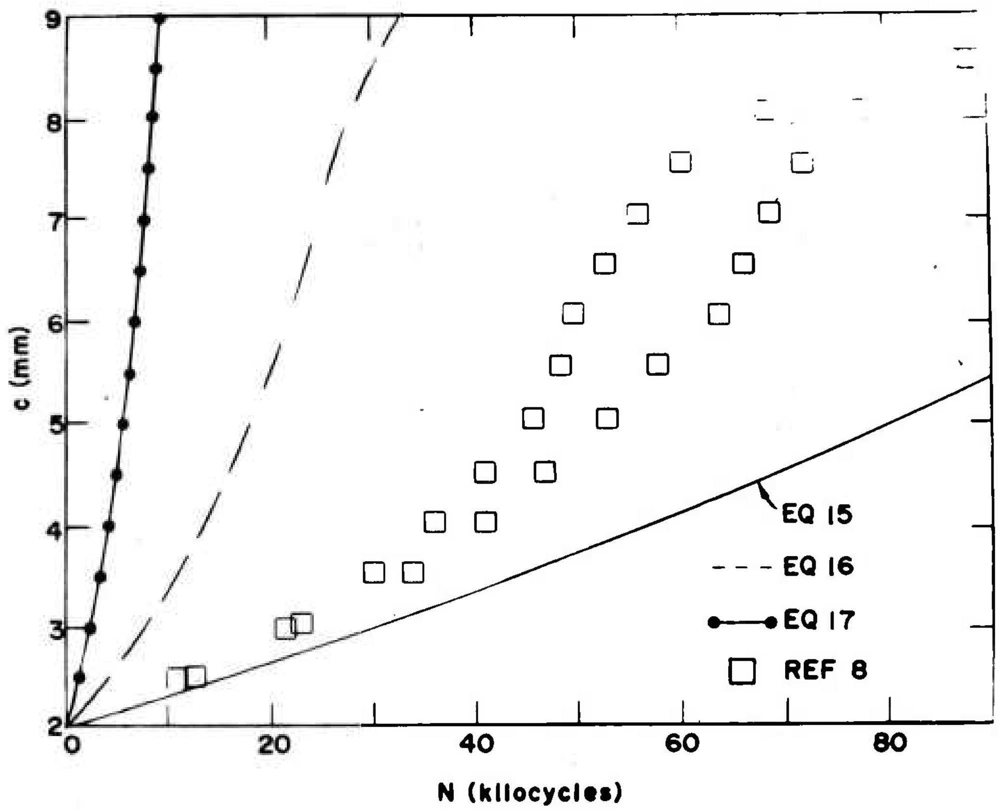


Figure 5. Comparison of Measured Fatigue Crack Growth and Predicted Fatigue Crack Growth Using Various Models for a Cylinder Containing 50 Percent Overstrain Residual Stresses.

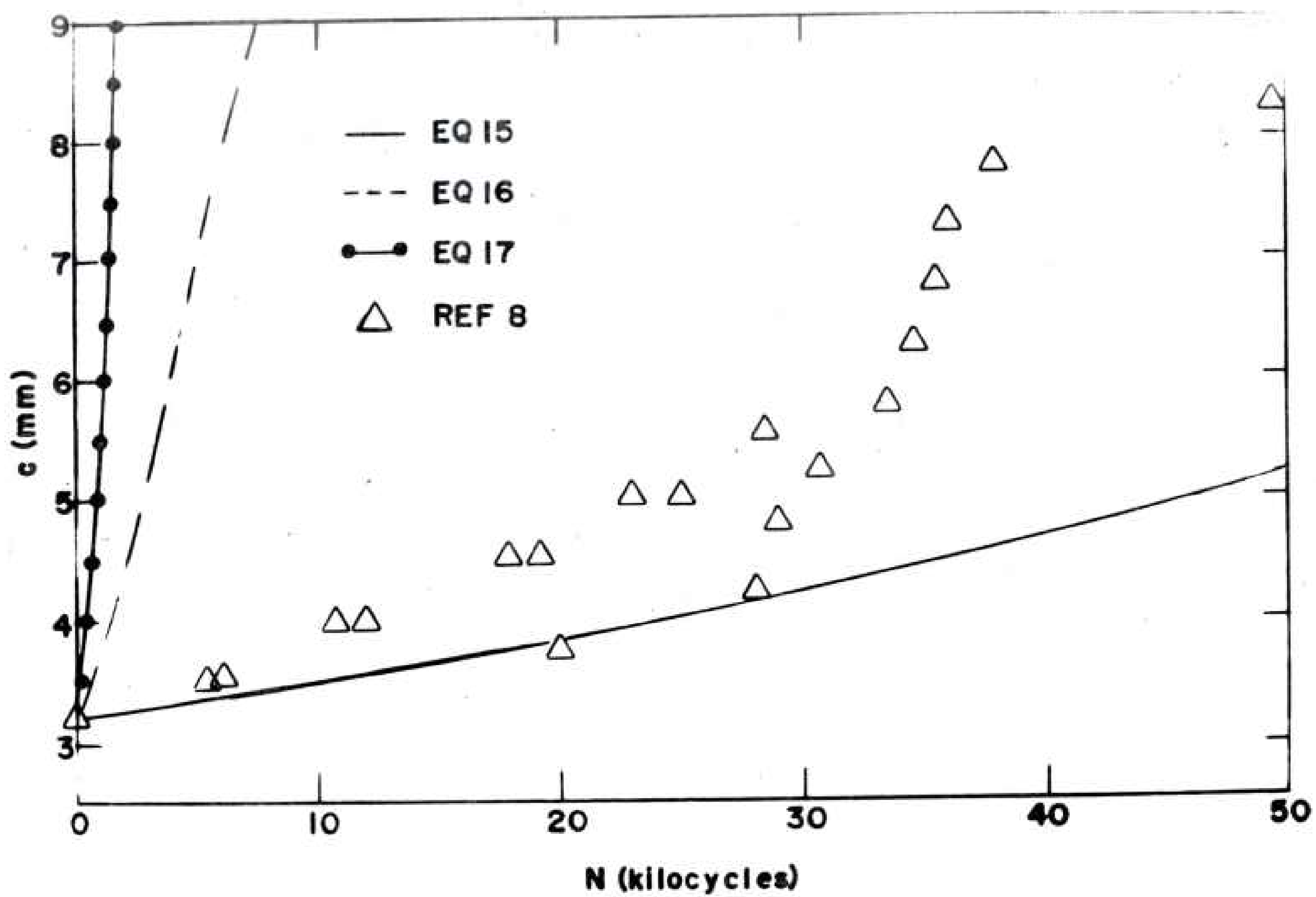


Figure 6. Comparison of Measured Fatigue Crack Growth and Predicted Fatigue Crack Growth Using Various Models for a Cylinder Containing 100 Percent Overstrain Residual Stress.

TECHNICAL REPORT INTERNAL DISTRIBUTION LIST

| | NO. OF COPIES |
|---|---|
| CHIEF, DEVELOPMENT ENGINEERING BRANCH | 1 |
| ATTN: DRDAR-LCB-DP | 1 |
| -DR | 1 |
| -DS (SYSTEMS) | 1 |
| -DS (ICAS GROUP) | 1 |
| -DC | 1 |
| CHIEF, ENGINEERING SUPPORT BRANCH | 1 |
| ATTN: DRDAR-LCB-SE | 1 |
| CHIEF, RESEARCH BRANCH | 2 |
| ATTN: DRDAR-LCB-R (ELLEN FOGARTY) | 1 |
| -RA | 1 |
| -RM | 1 |
| -RP | 1 |
| -RT | 1 |
| TECHNICAL LIBRARY<br>ATTN: DRDAR-LCB-TL | 5 |
| TECHNICAL PUBLICATIONS & EDITING UNIT<br>ATTN: DRDAR-LCB-TL | 2 |
| DIRECTOR, OPERATIONS DIRECTORATE | 1 |
| DIRECTOR, PROCUREMENT DIRECTORATE | 1 |
| DIRECTOR, PRODUCT ASSURANCE DIRECTORATE | 1 |

NOTE: PLEASE NOTIFY DIRECTOR, BENET WEAPONS LABORATORY, ATTN: DRDAR-LCB-TL, OF ANY REQUIRED CHANGES.

TECHNICAL REPORT EXTERNAL DISTRIBUTION LIST

| | NO. OF COPIES |
|---|---|
| ASST SEC OF THE ARMY<br>RESEARCH & DEVELOPMENT<br>ATTN: DEP FOR SCI & TECH<br>THE PENTAGON<br>WASHINGTON, D.C. 20315 | 1 |
| COMMANDER<br>DEFENSE TECHNICAL INFO CENTER<br>ATTN: DTIC-DDA<br>CAMERON STATION<br>ALEXANDRIA, VA 22314 | 12 |
| COMMANDER<br>US ARMY MAT DEV & READ COMD<br>ATTN: DRCDE-SG<br>5001 EISENHOWER AVE<br>ALEXANDRIA, VA 22333 | 1 |
| COMMANDER<br>US ARMY ARRADCOM<br>ATTN: DRDAR-LC | 1 |
| DRDAR-LCA (PLASTICS TECH EVAL CEN) | 1 |
| DRDAR-LCE | 1 |
| DRDAR-LCM (BLDG 321) | 1 |
| DRDAR-LCS | 1 |
| DRDAR-LCU | 1 |
| DRDAR-LCW | 1 |
| DRDAR-TSS (STINFO)<br>DOVER, NJ 07801 | 2 |
| DIRECTOR<br>US ARMY BALLISTIC RESEARCH LABORATORY<br>ATTN: DRDAR-TSB-S (STINFO)<br>ABERDEEN PROVING GROUND, MD 21005 | 1 |
| COMMANDER<br>US ARMY ARRCOM<br>ATTN: DRSAR-LEP-L<br>ROCK ISLAND ARSENAL<br>ROCK ISLAND, IL 61299 | 1 |
| COMMANDER<br>ROCK ISLAND ARSENAL<br>ATTN: SARRI-ENM (MAT SCI DIV)<br>ROCK ISLAND, IL 61299 | 1 |
| DIRECTOR<br>US ARMY INDUSTRIAL BASE ENG ACT<br>ATTN: DRXIB-M<br>ROCK ISLAND, IL 61299 | 1 |
| COMMANDER<br>US ARMY TANK-AUTMV R&D COMD<br>ATTN: TECH LIB - DRSTA-TSL<br>WARREN, MICHIGAN 48090 | 1 |
| COMMANDER<br>US ARMY TANK-AUTMV COMD<br>ATTN: DRSTA-RC<br>WARREN, MICHIGAN 48090 | 1 |
| COMMANDER<br>US MILITARY ACADEMY<br>ATTN: CHMN, MECH ENGR DEPT<br>WEST POINT, NY 10996 | 1 |
| US ARMY MISSILE COMD<br>REDSTONE SCIENTIFIC INFO CEN<br>ATTN: DOCUMENTS SECT, BLDG 4484<br>REDSTONE ARSENAL, AL 35898 | 2 |
| COMMANDER<br>US ARMY FGN SCIENCE & TECH CEN<br>ATTN: DRXST-SD<br>220 7TH STREET, N.E.<br>CHARLOTTESVILLE, VA 22901 | 1 |
| COMMANDER<br>US ARMY MATERIALS & MECHANICS RESEARCH CENTER<br>ATTN: TECH LIB - DRXMR-PL<br>WATERTOWN, MASS 02172 | 2 |

NOTE: PLEASE NOTIFY COMMANDER, ARRADCOM, ATTN: BENET WEAPONS LABORATORY, DRDAR-LCB-TL, WATERVLIET ARSENAL, WATERVLIET, N.Y. 12189, OF ANY REQUIRED CHANGES.

TECHNICAL REPORT EXTERNAL DISTRIBUTION LIST (CONT.)

| | NO. OF COPIES |
|---|---|
| COMMANDER<br>US ARMY RESEARCH OFFICE<br>ATTN: CHIEF, IPO<br>P.O. BOX 12211<br>RESEARCH TRIANGLE PARK, NC 27709 | 1 |
| COMMANDER<br>US ARMY HARRY DIAMOND LAB<br>ATTN: TECH LIB<br>2800 POWDER MILL ROAD<br>ADELPHIA, MD 20783 | 1 |
| COMMANDER<br>NAVAL SURFACE WEAPONS CEN<br>ATTN: TECHNICAL LIBRARY<br>CODE X212<br>DAHLGREN, VA 22448 | 1 |

| | NO. OF COPIES |
|---|---|
| DIRECTOR<br>US NAVAL RESEARCH LAB<br>ATTN: DIR, MECH DIV<br>CODE 26-27 (DOC LIB)<br>WASHINGTON, D.C. 20375 | 1<br>1 |
| METALS & CERAMICS INFO CEN<br>BATTELLE COLUMBUS LAB<br>505 KING AVE<br>COLUMBUS, OHIO 43201 | 1 |
| MATERIEL SYSTEMS ANALYSIS ACTV<br>ATTN: DRSXY-MP<br>ABERDEEN PROVING GROUND<br>MARYLAND 21005 | 1 |

NOTE: PLEASE NOTIFY COMMANDER, ARRADCOM, ATTN: BENET WEAPONS LABORATORY, DRDAR-LCB-TL, WATERVLIET ARSENAL, WATERVLIET, N.Y. 12189, OF ANY REQUIRED CHANGES.